AD-A157 866

AD

TECHNICAL REPORT ARLCB-TR-85018

TECHNICAL LIBRARY

STRESS INTENSITY FACTORS AT RADIAL CRACKS OF UNEQUAL DEPTH IN PARTIALLY AUTOFRETTAGED, PRESSURIZED CYLINDERS

S. L. PU

JUNE 1985

US ARMY ARMAMENT RESEARCH AND DEVELOPMENT CENTER
LARGE CALIBER WEAPON SYSTEMS LABORATORY
BENÉT WEAPONS LABORATORY
WATERVLIET N.Y. 12189

APPROVED FOR PUBLIC RELEASE; DISTRIBUTION UNLIMITED

DTIC QUALITY INSPECTED 3

DISCLAIMER

The findings in this report are not to be construed as an official Department of the Army position unless so designated by other authorized documents.

The use of trade name(s) and/or manufacture(s) does not constitute an official indorsement or approval.

DISPOSITION

Destroy this report when it is no longer needed. Do not return it to the originator.

SECURITY CLASSIFICATION OF THIS PAGE *(When Date Entered)*

REPORT DOCUMENTATION PAGE

READ INSTRUCTIONS BEFORE COMPLETING FORM

1. REPORT NUMBER: ARLCB-TR-85018	2. GOVT ACCESSION NO.
3. RECIPIENT'S CATALOG NUMBER	
4. TITLE *(and Subtitle)*: STRESS INTENSITY FACTORS AT RADIAL CRACKS OF UNEQUAL DEPTH IN PARTIALLY AUTOFRETTAGED, PRESSURIZED CYLINDERS	5. TYPE OF REPORT & PERIOD COVERED: Final
	6. PERFORMING ORG. REPORT NUMBER
7. AUTHOR(s): S. L. Pu	8. CONTRACT OR GRANT NUMBER(s)
9. PERFORMING ORGANIZATION NAME AND ADDRESS: US Army Armament Research & Development Center, Benet Weapons Laboratory, SMCAR-LCB-TL, Watervliet, NY 12189-5000	10. PROGRAM ELEMENT, PROJECT, TASK AREA & WORK UNIT NUMBERS: AMCMS No. 6111.02.H600.011, PRON No. 1A425M541A1A
11. CONTROLLING OFFICE NAME AND ADDRESS: US Army Armament Research & Development Center, Large Caliber Weapon Systems Laboratory, Dover, NJ 07801-5001	12. REPORT DATE: June 1985
	13. NUMBER OF PAGES: 24
14. MONITORING AGENCY NAME & ADDRESS *(if different from Controlling Office)*	15. SECURITY CLASS. *(of this report)*: UNCLASSIFIED
	15a. DECLASSIFICATION/DOWNGRADING SCHEDULE

16. DISTRIBUTION STATEMENT *(of this Report)*

Approved for public release; distribution unlimited.

17. DISTRIBUTION STATEMENT *(of the abstract entered in Block 20, if different from Report)*

18. SUPPLEMENTARY NOTES

19. KEY WORDS *(Continue on reverse side if necessary and identify by block number)*

Stress Intensity Factors
Multiple Cracks
Autofrettaged Cylinders
Cracks of Unequal Lengths
Fracture Mechanics

20. ABSTRACT *(Continue on reverse side if necessary and identify by block number)*

Stress intensity factors are estimated for radial cracks of unequal depths emanating from the inner surface of a partially autofrettaged cylinder subjected to various bore pressures. The approximate method developed for uneven radial cracks in a non-autofrettaged cylinder is applied to functional stress intensities. Linear superposition is then used to obtain the final stress intensity factors of uneven cracks due to a stress field which varies

(CONT'D ON REVERSE)

DD FORM 1 JAN 73 1473 EDITION OF 1 NOV 65 IS OBSOLETE

UNCLASSIFIED

SECURITY CLASSIFICATION OF THIS PAGE *(When Date Entered)*

20. ABSTRACT (CONT'D)

with the magnitude of bore pressure, the degree of autofrettage, and the elastic-plastic behavior of the cylinder material. The autofrettage residual stress reduces the level of stress intensity factors at inner radial cracks due to internal pressure, but has little effect on variations in stress intensity factors caused by changes in crack depths.

TABLE OF CONTENTS

TABLES

LIST OF ILLUSTRATIONS

INTRODUCTION

The linear fracture mechanics problem of a pressurized cylinder with many radial cracks has been extensively studied in recent years by a number of investigators. In earlier works, cracks were assumed to be uniformly distributed and of equal depths so the problem remained axisymmetric. In a recent report (ref 1), radial cracks of unequal depths were considered. It was found that the variation in stress intensity factor at a crack tip due to crack depth change of the same crack or another crack is approximately linear. A simple numerical method was used in Reference 1 to accurately estimate stress intensity factors at radial cracks of unequal depths in a pressurized, non-autofrettaged cylinder.

For a partially autofrettaged cylinder, the functional stress intensity approach was developed (ref 2) for equal depth radial cracks. The same approach can be extended to radial cracks of unequal depths. The functional stress intensity factors for uneven cracks must be first obtained by the numerical method developed in Reference 1. A combination of methods described in References 1 and 2 can be used to estimate stress intensity factors at uneven radial cracks in a pressurized, partially autofrettaged cylinder. Numerical results are given for two diametrically opposite cracks with crack length ratio varying from 0.7 to 1.4 for a thick-walled cylinder of wall ratio W = 2. The method, however, is general for a multi-crack configuration.

---

[1]Pu, S. L., "Stress Intensity Factors For a Circular Ring With Uniform Array of Radial Cracks of Unequal Depth," ARDC Technical Report No. ARLCB-TR-84021, Benet Weapons Laboratory, Watervliet, NY, June 1984.

[2]Pu, S. L., "A Functional Stress Intensity Approach to Multiply-Cracked, Partially Autofrettaged Cylinders," Transactions of the 28th Conference of Army Mathematicians, ARO Report 83-1, 1983, pp. 263-283.

RESIDUAL STRESSES IN AN AUTOFRETTAGED CYLINDER

It is now a routine procedure to autofrettage a cannon tube to introduce residual compressive stress in the circumferential direction near the bore to slow the growth of radial cracks which occur after repeated firing. The residual stress distribution is difficult to measure and can only be estimated by theoretical prediction based on various assumptions of material models. From a recent paper (ref 3), it is assumed that the residual stresses can be closely approximated by the following expressions:

$$\sigma_r(r)/\sigma_o = \begin{cases} A_r + B_r/r^2 + C_r \ell nr & 1 \leq r \leq 1+\varepsilon t \quad (1) \\ D_r + E_r/r^2 & 1+\varepsilon t \leq r \leq W \quad (2) \end{cases}$$

$$\sigma_\theta(r)/\sigma_o = \begin{cases} A_\theta + B_\theta/r^2 + C_\theta \ell nr & 1 \leq r \leq 1+\varepsilon t \quad (3) \\ D_\theta + E_\theta/r^2 & 1+\varepsilon t \leq r \leq W \quad (4) \end{cases}$$

where (r,θ) are polar coordinates with origin at the center of the cylinder. The inner radius is taken as the length unit. The outer radius is then equal to the wall ratio W. The wall thickness t equals W-1. The degree of autofrettage ε is defined by $\varepsilon = (r_p-1)/t$ where r_p is the radius of elastic-plastic interface during pressurization in an autofrettage procedure. σ_o is the yield stress of the material and σ_r, σ_θ are stress components in r and θ-directions, respectively. The superposition coefficients $A_r,\ldots,E_r$, and $A_\theta,\ldots,E_\theta$, vary with W, ε, and the material model used. For a highly idealized material which obeys von Mises' criterion and is incompressible and elastic-perfectly plastic, and for the cylinder which is under a state of

---

[3]Pu, S. L. and Chen, P. C. T., "Stress Intensity Factors For Radial Cracks in a Pre-stressed, Thick-Walled Cylinder of Strain-Hardening Materials," J. of Pressure Vessel Technology, Vol. 105, 1983, pp. 117-123.

plane strain, we conclude from Reference 4 that:

$$A_\theta = \frac{1}{\sqrt{3}} [2 - P_1(\varepsilon)] \quad , \quad B_\theta = \frac{-1}{\sqrt{3}} P_1(\varepsilon) \quad , \quad C_\theta = \frac{2}{\sqrt{3}} \tag{5}$$

$$D_\theta = \frac{1}{\sqrt{3}\, W^2} [(1+\varepsilon t)^2 - P_1(\varepsilon)] \quad , \quad E_\theta = \frac{1}{\sqrt{3}} [(1+\varepsilon t)^2 - P_1(\varepsilon)] \tag{6}$$

where

$$P_1(\varepsilon) = \frac{w^2}{w^2-1} \left[1 - \frac{(1+\varepsilon t)^2}{w^2} + 2\ell n(1+\varepsilon t)\right] \tag{7}$$

For a less restrictive material model which behaves more closely to high strength steels of pressure vessels, residual stresses are usually obtained by numerical methods and are given by numerical values at discrete points. The superposition coefficients are a set of constants found by the least squares method. In a specific example (ref 3), the material is assumed to have ν = 0.3, E_t/E = 0.1 where E_t is the tangent-modulus of a strain-hardening material, and the material follows the incremental plastic stress-strain relation of Prandtl-Reuss and the yield criterion of von Mises in the plastic region. The numerical residual stresses obtained by Chen (ref 5) using the finite difference method for a cylinder of W = 2 can be closely approximated by A_θ = 0.170, B_θ = 1.030, and C_θ = 0.890 for ε = 1 and by a different set of superposition coefficients for a different value of ε. The corresponding coefficients from Eqs. (5) and (7) for idealized materials for W = 2, ε = 1

---

[3]Pu, S. L. and Chen, P. C. T., "Stress Intensity Factors For Radial Cracks in a Pre-stressed, Thick-Walled Cylinder of Strain-Hardening Materials," J. of Pressure Vessel Technology, Vol. 105, 1983, pp. 117-123.

[4]Hill, R., The Mathematical Theory of Plasticity, Oxford at the Clarendon Press, 1950.

[5]Chen, P. C. T., "Numerical Prediction of Residual Stresses in an Autofrettaged Tube of Compressible Material," Proceedings of the 1981 Army Numerical Analysis and Computer Conference, pp. 351-362.

are $A_\theta = 0.0875$, $B_\theta = -1.067$, and $C_\theta = 1.155$ which are quite different from the coefficients for the strain-hardening material given previously.

The underlying concept here is that the residual stresses in a partially autofrettaged cylinder, without reverse yielding during elastic unloading, can be closely approximated by expressions of Eqs. (1) through (4). Once the superposition coefficients are found, then the effect of such residual stresses on stress intensity factors at radial cracks in the cylinder can be estimated.

FUNCTIONAL STRESS INTENSITIES

According to the weight function method (refs 6,7), the mode I stress intensity factor due to a symmetrical load system 2 can be found if the mode I stress intensity factor K* and displacement field $\underset{\sim}{u}^*$ associated with the symmetric load system 1 for the same cracked geometry are known. For radially cracked rings, this method gives:

$$K = \frac{H}{K^*} \int_o^a p_c(x) \frac{\partial v^*}{\partial a} dx \qquad (8)$$

where a is the crack length, x is a distance measured along the crack from the base toward the tip, v^* is the normal component of crack face displacement, $H = E$ for plane stress and $H = E/(1-\nu^2)$ for plane strain, and $p_c(x)$ is the crack face pressure which can be found from the hoop stress in an uncracked ring subjected to the symmetric load of interest.

Taking the right side of Eq. (3) as $p_c(x)$ into Eq. (8) with $r = 1+x$, we

---

[6]Bueckner, H. F., "A Novel Principle for the Computation of Stress Intensity Factors," Z. Agnew. Math. Mech., Vol. 50, 1970, pp. 529-546.

[7]Rice, J. R., "Some Remarks on Elastic Crack-Tip Stress Fields," Int. Journal of Solids and Structures, Vol. 8, 1972, pp. 751-758.

have:

$$\frac{K(\varepsilon)}{\sigma_o} = A_\theta K(1) + B_\theta K(r^{-2}) + C_\theta K(\ell nr) \tag{9}$$

where $K(\varepsilon)$ is the mode I stress intensity factor at a radial crack emanating from the bore with crack length $c \leq \varepsilon t$ in a stress field given by the residual stress, Eq. (3), and $K(1)$, $K(r^{-2})$, and $K(\ell nr)$ are integrals given by Eq. (8) with $p_c(x) = 1$, $(1+x)^{-2}$ and $\ell n(1+x)$, respectively. These integrals are stress intensity factors associated with the specific crack face loadings. They are basic quantities and are named functional stress intensities.

One way to find functional stress intensity factors is to assume ν^* as a function of a and x and perform the integration of Eq. (8). An approximation by assuming ν^* as a conic section is given by Grandt (ref 8). A way to deviate from this approach is given in Reference 2 by using finite element computations of stress intensity factors of the cracked cylinder subjected to the following three loadings. The hook stress in an uncracked cylinder under internal pressure p_i is:

$$\frac{\sigma_\theta}{p_i} = \frac{1}{W^2-1}\left(1 + \frac{W^2}{r^2}\right) \tag{10}$$

The stress intensity factor produced by this stress acting on the crack face is:

$$\frac{K(p_i)}{P_i} = \frac{1}{W^2-1} K(1) + \frac{W^2}{W^2-1} K(r^{-2}) \tag{11}$$

---

[2]Pu, S. L., "A Functional Stress Intensity Approach to Multiply-Cracked, Partially Autofrettaged Cylinders," Transactions of the 28th Conference of Army Mathematicians, ARO Report 83-1, 1983, pp. 263-283.

[8]Grandt, A. F., "Stress Intensity Factors for Through-Cracked Fastener Holes," Int. Journal of Fracture, Vol. 11, 1975, pp. 283-294.

Similarly, the stress intensity factor due to a uniform tension p_o on the outer cylindrical surface is:

$$\frac{K(p_o)}{p_o} = \frac{W^2}{W^2-1} K(1) + \frac{W^2}{W^2-1} K(r^{-2}) \qquad (12)$$

The left-hand sides of Eqs. (11) and (12) are calculated from two separate finite element computations. The functional stress intensity factors K(1) and $K(r^{-2})$ are solved from Eqs. (11) and (12). The third finite element computation which supplies values to the left-hand side of Eq. (9) is obtained by applying an axisymmetrical thermal loading to the cylinder.

$$T(r) = T_o - (T_o - T_W) \ell n(\frac{r}{W}) \qquad 1 \leq r \leq W \qquad (13)$$

where T_o is the temperature at the bore and T_W is the temperature at the outer cylindrical surface. Temperature gradient is related to material constants by:

$$T_o - T_W = \frac{4\sigma_o}{\sqrt{3}} \frac{(1-\nu) \ell nW}{E\alpha} \qquad (14)$$

where E and α are Young's modulus and the coefficient of linear thermal expansion, respectively. The thermal stresses produced by the loading given by Eq. (13) are identical to the fully autofrettaged residual stresses in Eqs. (1) through (4) with superposition coefficients given by Eqs. (5) and (6); see Reference 9. The only unknown K(ℓnr) in Eq. (9) can be easily solved.

---

[9]Hussain, M. A., Pu, S. L., Vasilakis, J. D., and O'Hara, P., "Simulation of Partial Autofrettage by Thermal Loads," Journal of Pressure Vessel Technology, Vol. 102, No. 3, 1980, pp. 314-318.

RADIAL CRACKS OF UNEQUAL DEPTHS

For non-autofrettaged cylinders, an approximate method is described in Reference 1 to estimate stress intensity factors at radial cracks of uneven depths. Finite element code APES is used to obtain changes in stress intensity factors at different crack tips due to a systematic change in crack length of a radial crack. The total change in stress intensity factor at a particular crack due to simultaneous changes in crack lengths of all radial cracks is approximately the sum of changes in stress intensity factor at that crack due to crack length changes, one at a time.

For partially autofrettaged cylinders with radial cracks of equal depth, we use functional stress intensities defined previously as basic quantitites. The final stress intensity factor is given by a linear superposition of functional stress intensities such as Eq. (9). The superposition coefficients are known from the residual stress solution and the Lame´ solution. For radial cracks of unequal depths, the approximate method developed in Reference 1 is applied to each functional stress intensity factor. Once changes in all functional stress intensity factors are known due to simultaneous changes in crack lengths of radial cracks, the superposition formula can be used to estimate the final stress intensity factor at each crack tip in a partially autofrettaged and pressurized cylinder with uniform array of radial cracks of unequal depths.

---

[1]Pu, S. L., "Stress Intensity Factors For a Circular Ring With Uniform Array of Radial Cracks of Unequal Depth," ARDC Technical Report No. ARLCB-TR-84021, Benet Weapons Laboratory, Watervliet, NY, June 1984.

NUMERICAL RESULTS AND DISCUSSIONS

Using two diametrically opposite cracks as an example, the stress intensity factor is plotted as a function of crack depth in Figure 1 for an equal crack configuration of a non-autofrettaged cylinder of W = 2 subjected to a uniform tension p on the outer cylindrical surface. In the same figure, results of n = 1, 3, 4, 6 are also shown to indicate that stress intensity factor for n = 2 is the highest at a given crack depth c. The subscript e is used to emphasize that the quantity is of equal crack depth configuration. In Figure 2, the change in stress intensity ratio is plotted as a function of change in crack depth when one of the cracks is growing from the equal depth to an unequal depth configuration. To distinguish one crack from other cracks in an unequal depth configuration, an arbitrary numbering system is used. Quantities with a subscript 1, such as K_1 and c_1, are the ones associated with crack 1. Dimensionless stress intensity factor and crack depth are defined by $N_i = K_i/K_e$ and $\rho_i = c_i/c$. The changes in N and ρ are designated by $\Delta N_i = (K_i - K_e)/K_e$ and $\Delta\rho_i = (c_i - c)/c$.

For partially autofrettaged cylinders, functional stress intensity factors are studied as basic quantities. Figure 3 shows functional stress intensity factors as functions of crack depth when two radial cracks are of equal depths. Results in Figure 3 are used to normalize functional stress intensities when radial cracks are of unequal depths. Figures 4 through 6, similar to Figure 2 of non-autofrettaged cylinders, are graphs of ΔN_i versus $\Delta\rho_1$ for the three basic functional stress intensities corresponding to normal crack face loadings $p_c = 1$, $1/r^2$, and ℓnr, respectively.

Using the approximate method described in Reference 1 and the results in Figures 4 through 6, functional stress intensity factors can be estimated for unequal depth radial cracks. The approximate results agree well with results directly calculated from finite element computations. For instance, for n = 2, $c_2 = c = 0.2$ and c_1 varies from 0.14 to 0.28. A comparison of approximate and finite element results of functional stress intensities is given in Table I.

TABLE I. APPROXIMATE VS. FINITE ELEMENT RESULTS OF $K_i(p_c)/K_e(p_c)$ FOR W = 2, n = 2, c = 0.2, $\rho_1 = 0.7$ and $\rho_1 = 1.4$

		$c_2 = 0.2$, $\rho_1 = 0.7$		$c_2 = 0.2$, $\rho_1 = 1.4$	
i	pc	Approximate	F.E.	Approximate	F.E.
1	1	0.8113	0.8130	1.2515	1.2519
	r^{-2}	0.8734	0.8622	1.1688	1.1653
	ℓnr	0.5082	0.5698	1.6557	1.6797
2	1	0.9629	0.9710	1.0495	1.0519
	r^{-2}	0.9643	0.9706	1.0477	1.0495
	ℓnr	0.9574	0.9473	1.0568	1.0617

Knowing $K_i(p_c)/K_e(p_c)$ and $K_e(p_c)$, Figure 3, then Eq. (9) can be used to compute stress intensity factors at radial cracks of unequal depths corresponding to a residual stress distribution of Eq. (3). The superposition coefficients are known from the residual stress distribution. For the

---

[1] Pu, S. L., "Stress Intensity Factors For a Circular Ring With Uniform Array of Radial Cracks of Unequal Depth," ARDC Technical Report No. ARLCB-TR-84021, Benet Weapons Laboratory, Watervliet, NY, June 1984.

idealized material model, they are given by Eq. (5). Let $\varepsilon = 1.0$ and 0.6; then numerical values of $K_i(\varepsilon)/(\sigma_o\sqrt{R_1})$ are obtained by the approximate method and the finite element method. The results are compared in Table II. The negative sign indicates that the effect of autofrettage residual stress on inner cracks is to resist crack opening due to internal pressure or other loadings. The resistance varies and never exceeds the crack opening force. The values in Table II are the maximum resistance. The stress intensity factor at a crack remains zero unless the crack opening force is larger than the maximum resistance given by the residual stress distribution.

TABLE II. APPROXIMATE VS. FINITE ELEMENT RESULTS OF $K_i(\varepsilon)/(\sigma_o R_1^{1/2})$ FOR $W = 2$, $n = 2$, $c = 0.2$, $\rho_1 = 0.7$ and $\rho_1 = 1.4$

		$c_2 = 0.2$, $\rho_1 = 0.7$		$c_2 = 0.2$, $\rho_1 = 1.4$	
i	ε	Approximate	F.E.	Approximate	F.E.
1	1.0	-0.6201	-0.6001	-0.6938	-0.6879
	0.6	-0.5236	-0.5040	-0.5545	-0.5486
2	1.0	-0.6294	-0.6320	-0.6814	-0.6822
	0.6	-0.5187	-0.5205	-0.5610	-0.5615

For an inner cracked, partially autofrettaged cylinder subject to an internal pressure p, the resultant stress intensity factor is the sum of Eqs. (9) and (12). If p is σ_o/f where f is a constant, the resultant stress intensity factor at crack i is given in terms of functional stress intensity factors by:

$$\frac{K_i(p,\varepsilon)}{\sigma_o\sqrt{R_1}} = \left(A_\theta(\varepsilon) + \frac{W^2}{f(W^2-1)}\right)\frac{K_i(1)}{\sqrt{R_1}} + \left(B_\theta(\varepsilon) + \frac{W^2}{f(W^2-1)}\right)\frac{K_i(r^{-2})}{\sqrt{R_1}} + C_\theta(\varepsilon)\frac{K_i(\ell nr)}{\sqrt{R_1}} \tag{15}$$

Normalizing $K_i(p,\varepsilon)$ by $K_e(p,\varepsilon=0)$, numerical results for i = 1 or 2, ε = 0.5 or 1, and f = 1.5 or 3 are shown in Figures 7 through 9 for c = 0.1, 0.2, and 0.3, respectively. In these figures, the superposition coefficients A_θ, B_θ, and C_θ are given by Eq. (5). For a strain-hardening material with tangent modulus E_t = 0.1E, the residual stress distributions obtained by Chen (ref 5) were closely approximated by various sets of superposition coefficients in Reference 3. Using those, the final stress intensity factors ratios are shown in solid lines in Figure 10 in comparison with broken lines for idealized materials.

In Figures 7 through 9, all lines with the same i are nearly parallel, which indicates that the effect of autofrettage residual stress is simply a proportional reduction of stress intensity factor. The same trend is true in Figure 10 for strain-hardening material. The resistance to crack opening due to autofrettage is slightly reduced in strain-hardening material than in the idealized material (ref 3). This reduction is in proportion to the change in crack depths so the solid lines remain parallel to the broken lines in Figure 10.

---

[3]Pu, S. L. and Chen, P. C. T., "Stress Intensity Factors For Radial Cracks in a Pre-stressed, Thick-Walled Cylinder of Strain-Hardening Materials," J. of Pressure Vessel Technology, Vol. 105, 1983, pp. 117-123.

[5]Chen, P. C. T., "Numerical Prediction of Residual Stresses in an Autofrettaged Tube of Compressible Material," Proceedings of the 1981 Army Numerical Analysis and Computer Conference, pp. 351-362.

REFERENCES

1. Pu, S. L., "Stress Intensity Factors For a Circular Ring With Uniform Array of Radial Cracks of Unequal Depth," ARDC Technical Report No. ARLCB-TR-84021, Benet Weapons Laboratory, Watervliet, NY, June 1984.

2. Pu, S. L., "A Functional Stress Intensity Approach to Multiply-Cracked, Partially Autofrettaged Cylinders," Transactions of the 28th Conference of Army Mathematicians, ARO Report 83-1, 1983, pp. 263-283.

3. Pu, S. L. and Chen, P. C. T., "Stress Intensity Factors For Radial Cracks in a Pre-stressed, Thick-Walled Cylinder of Strain-Hardening Materials," J. of Pressure Vessel Technology, Vol. 105, 1983, pp. 117-123.

4. Hill, R., The Mathematical Theory of Plasticity, Oxford at the Clarendon Press, 1950.

5. Chen, P. C. T., "Numerical Prediction of Residual Stresses in an Autofrettaged Tube of Compressible Material," Proceedings of the 1981 Army Numerical Analysis and Computer Conference, pp. 351-362.

6. Bueckner, H. F., "A Novel Principle for the Computation of Stress Intensity Factors," Z. Agnew. Math. Mech., Vol. 50, 1970, pp. 529-546.

7. Rice, J. R., "Some Remarks on Elastic Crack-Tip Stress Fields," Int. Journal of Solids and Structures, Vol. 8, 1972, pp. 751-758.

8. Grandt, A. F., "Stress Intensity Factors for Through-Cracked Fastener Holes," Int. Journal of Fracture, Vol. 11, 1975, pp. 283-294.

9. Hussain, M. A., Pu, S. L., Vasilakis, J. D., and O'Hara, P., "Simulation of Partial Autofrettage by Thermal Loads," Journal of Pressure Vessel Technology, Vol. 102, No. 3, 1980, pp. 314-318.

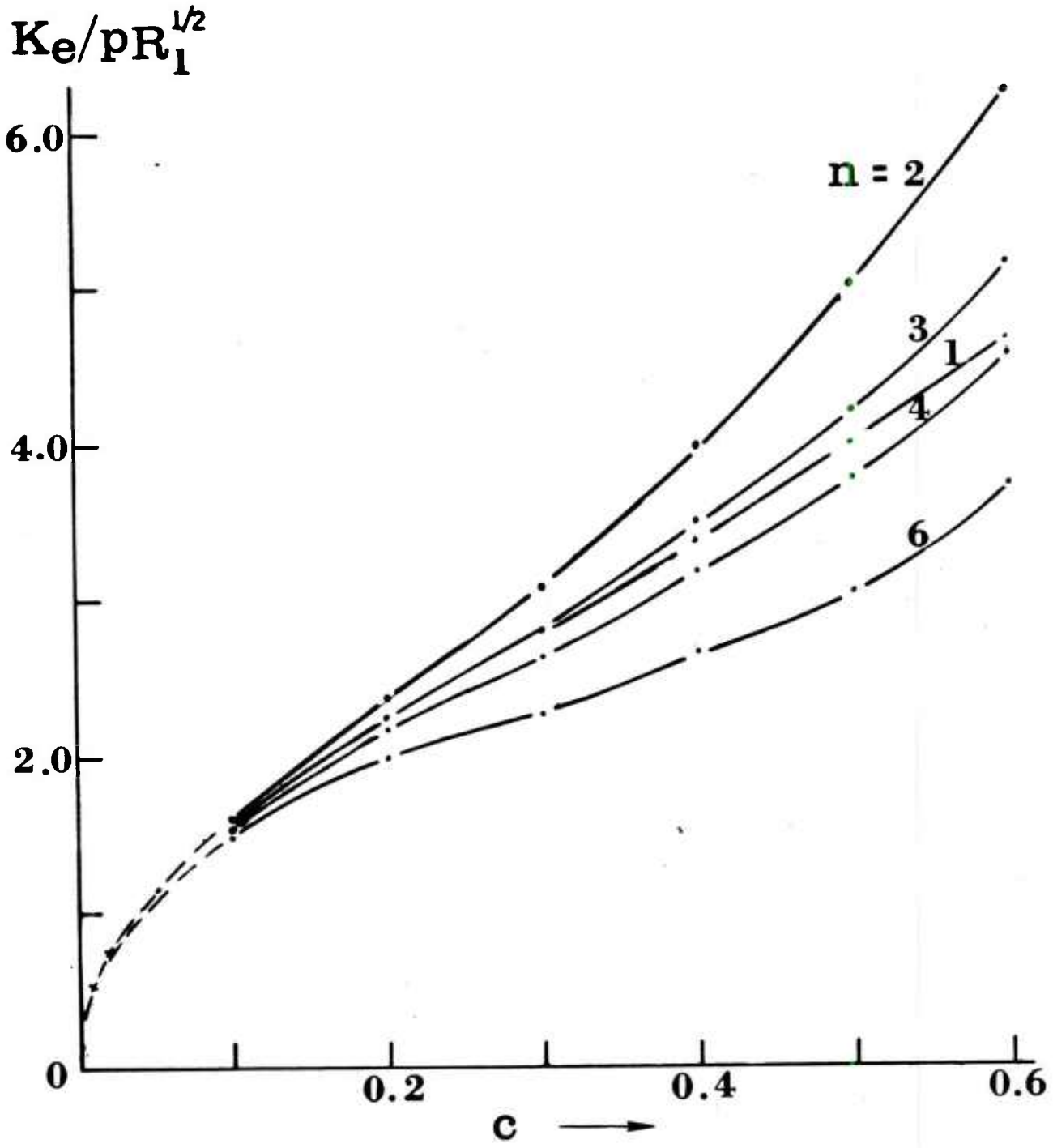

Figure 1. Stress intensity factors as a function of crack depth for a pressurized, non-autofrettaged cylinder of W = 2 with n cracks of equal depths. Dots are finite element results.

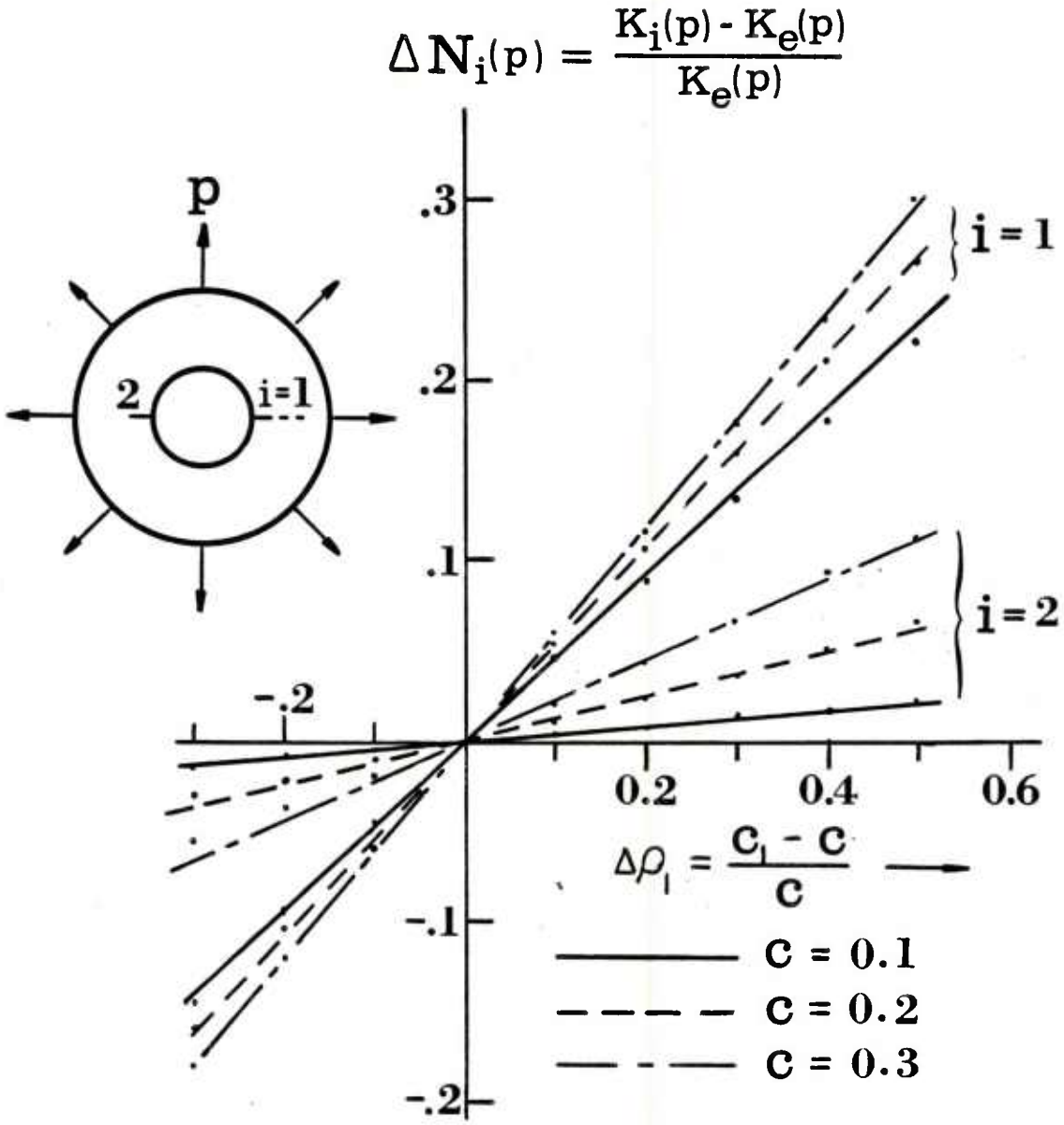

Figure 2. Changes in stress intensity ratio as a function of relative change in one of the crack depths for pressurized cylinder with two diametrically opposite cracks. Dots are finite element results.

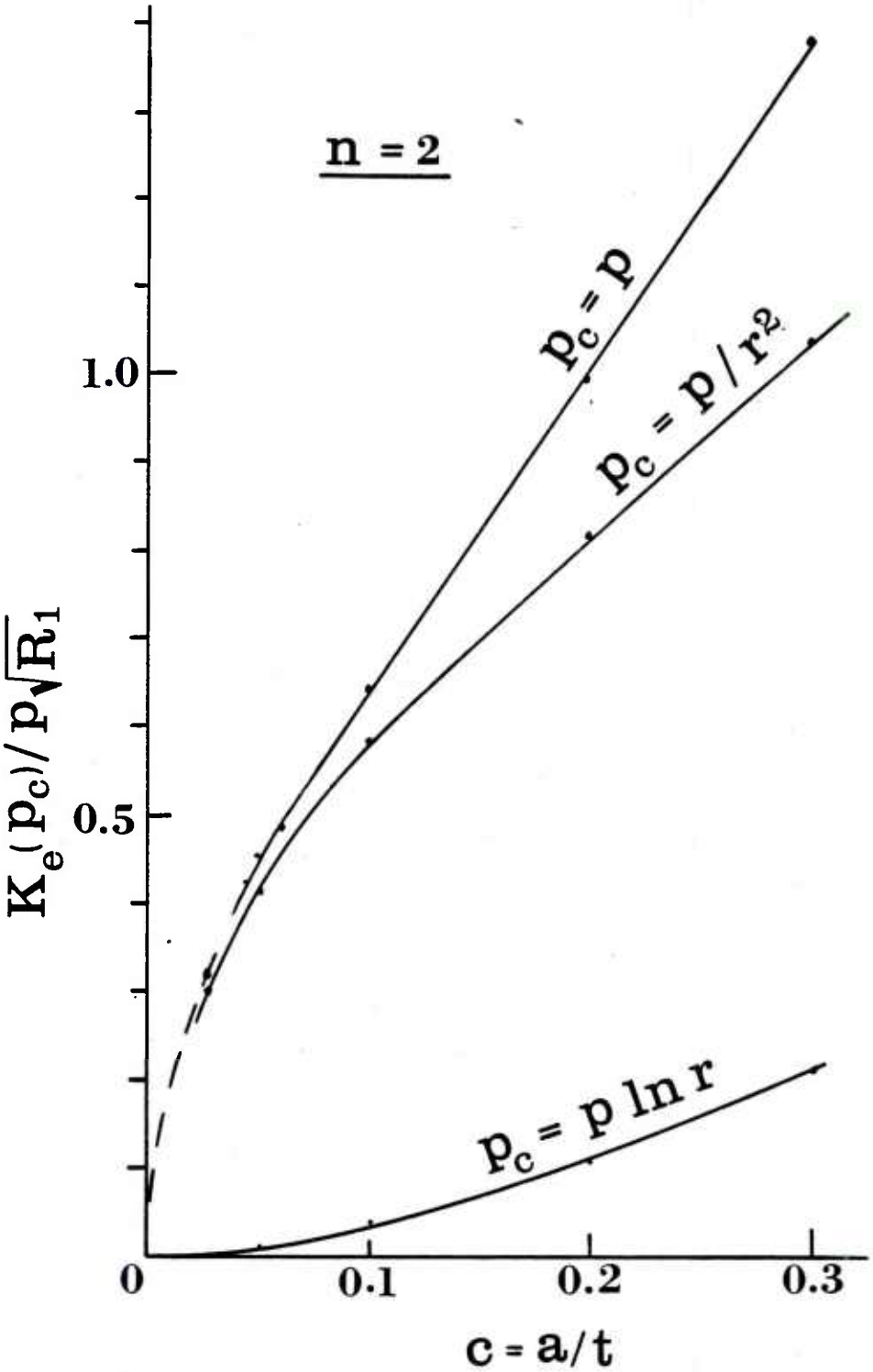

Figure 3. Functional stress intensity factors as a function of crack depth for two equal cracks under three types of basic crack face loadings. Dots are finite element results.

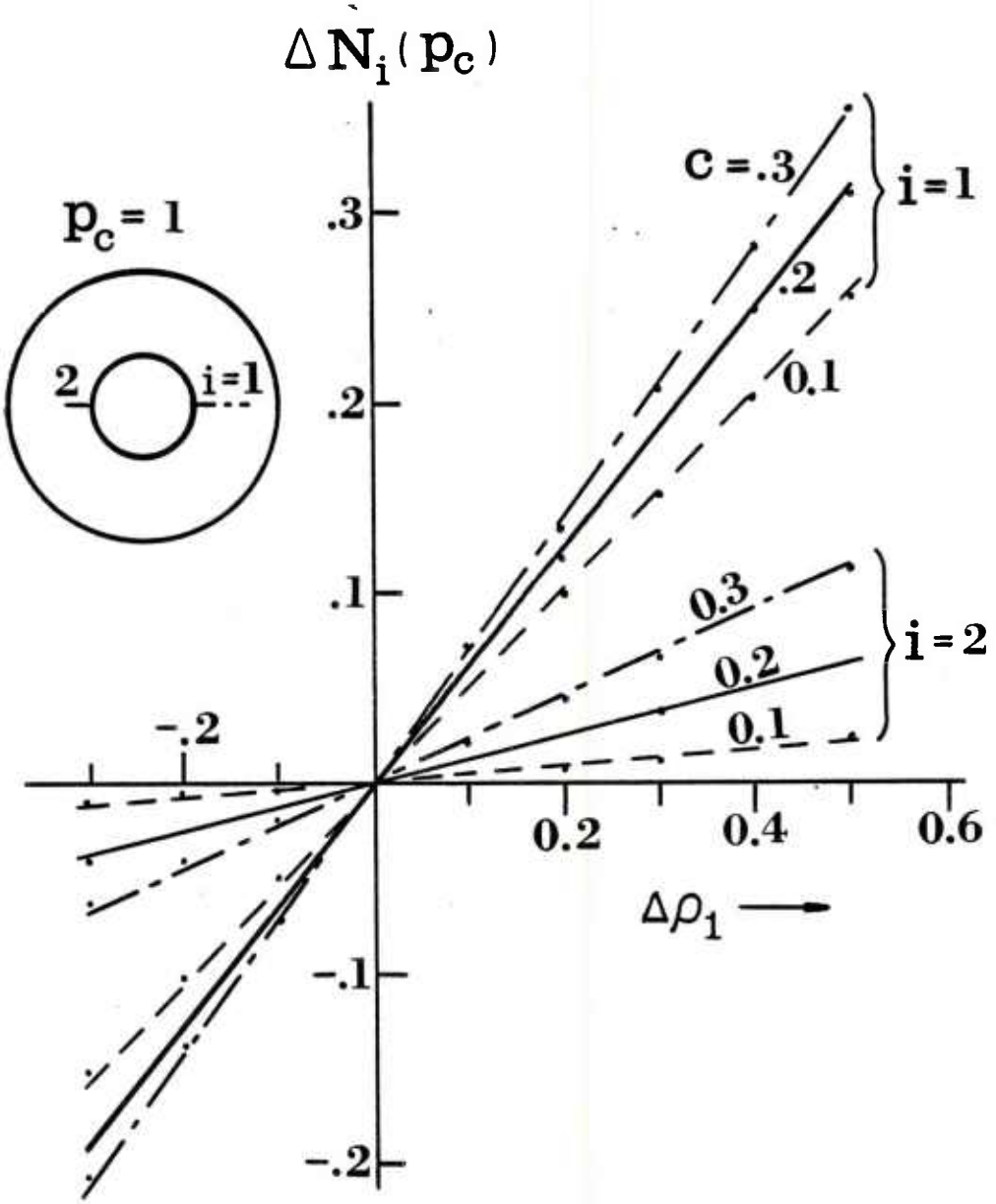

Figure 4. Changes in stress intensity ratio as a function of relative change in one of the crack depths for a two-crack configuration due to a constant crack face loading. Dots are finite element results.

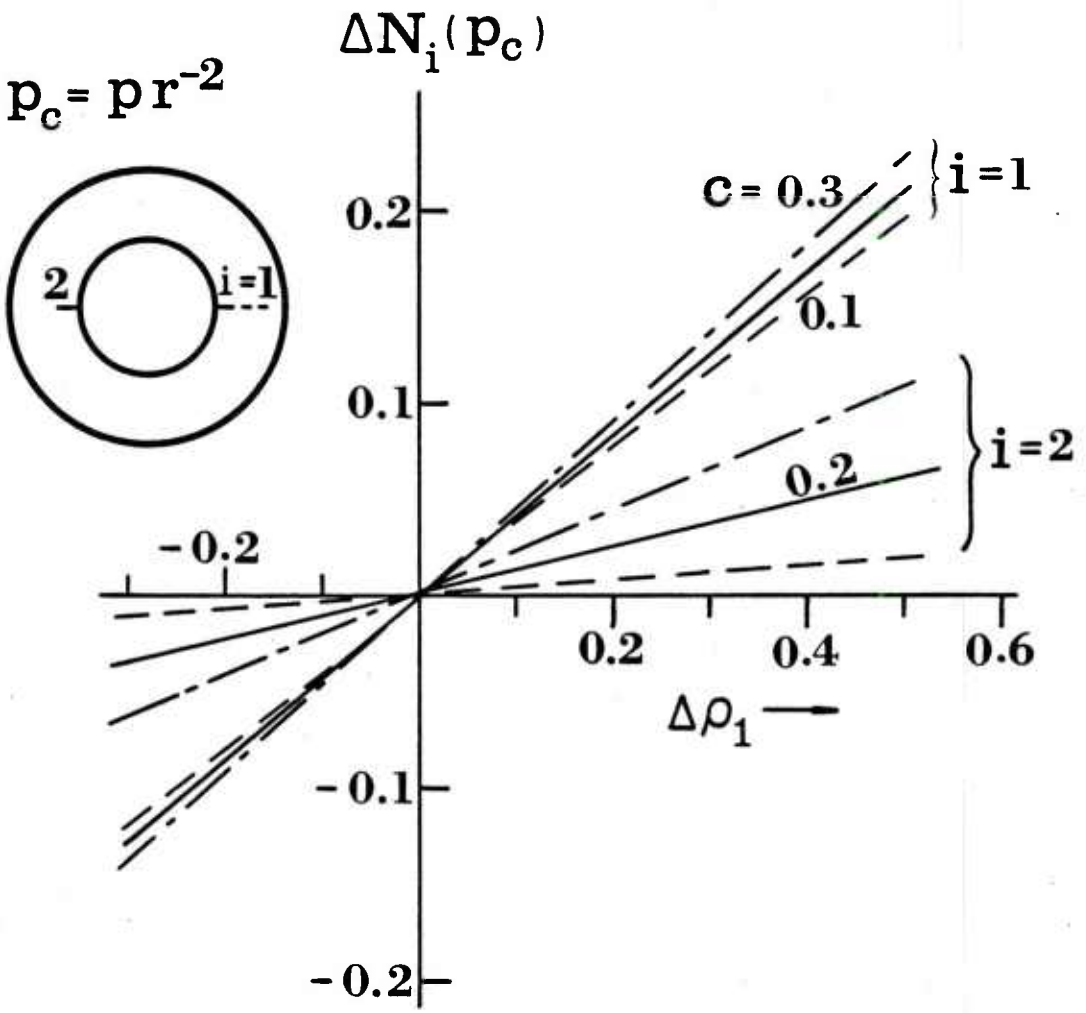

Figure 5. Changes in stress intensity ratio as a function of relative change in one of the crack depths for a two-crack configuration due to a crack face loading of pr^{-2}.

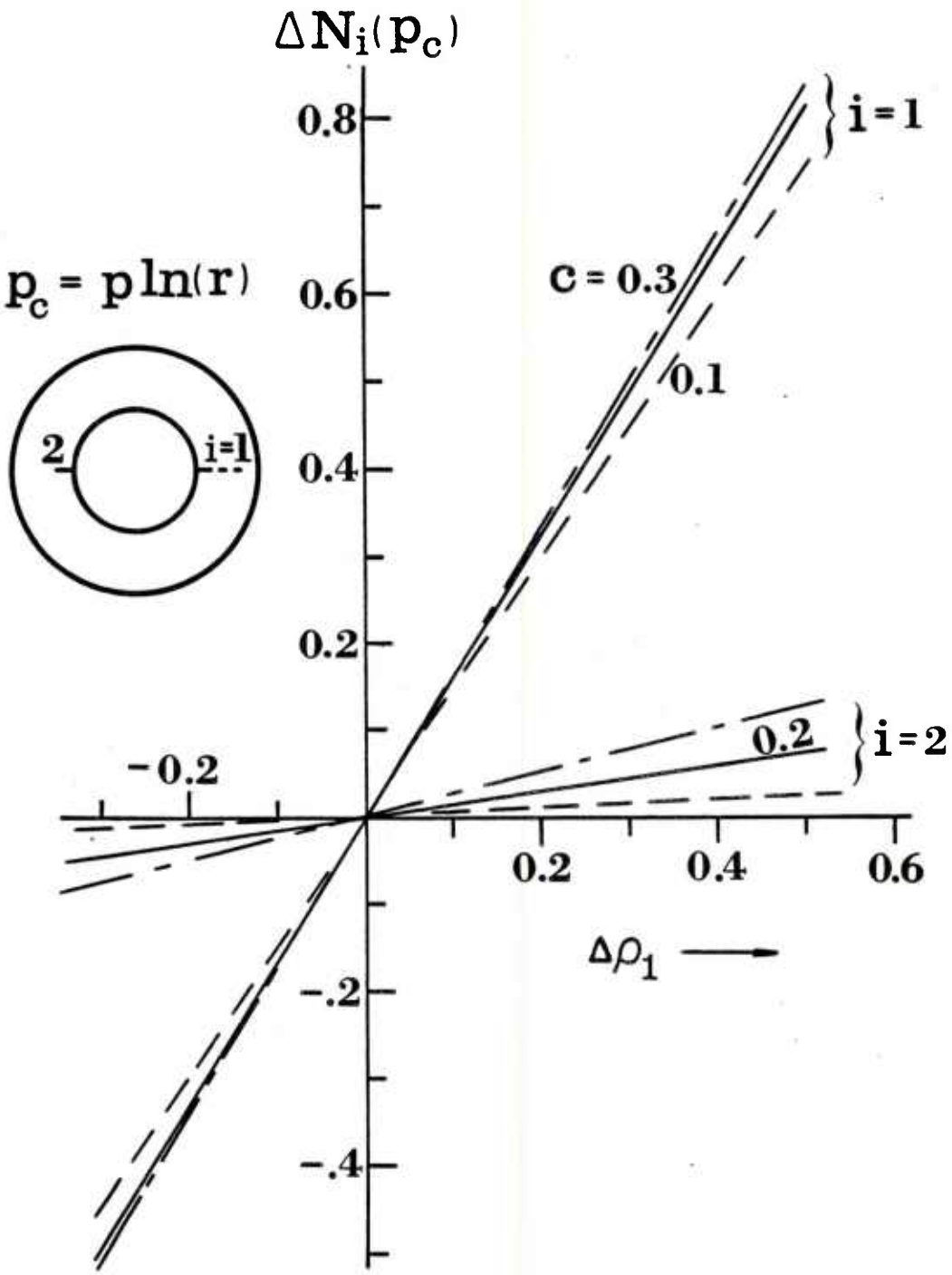

Figure 6. Changes in stress intensity ratio as a function of relative change in one of the crack depths for a two-crack configuration due to a crack face loading of pln(r).

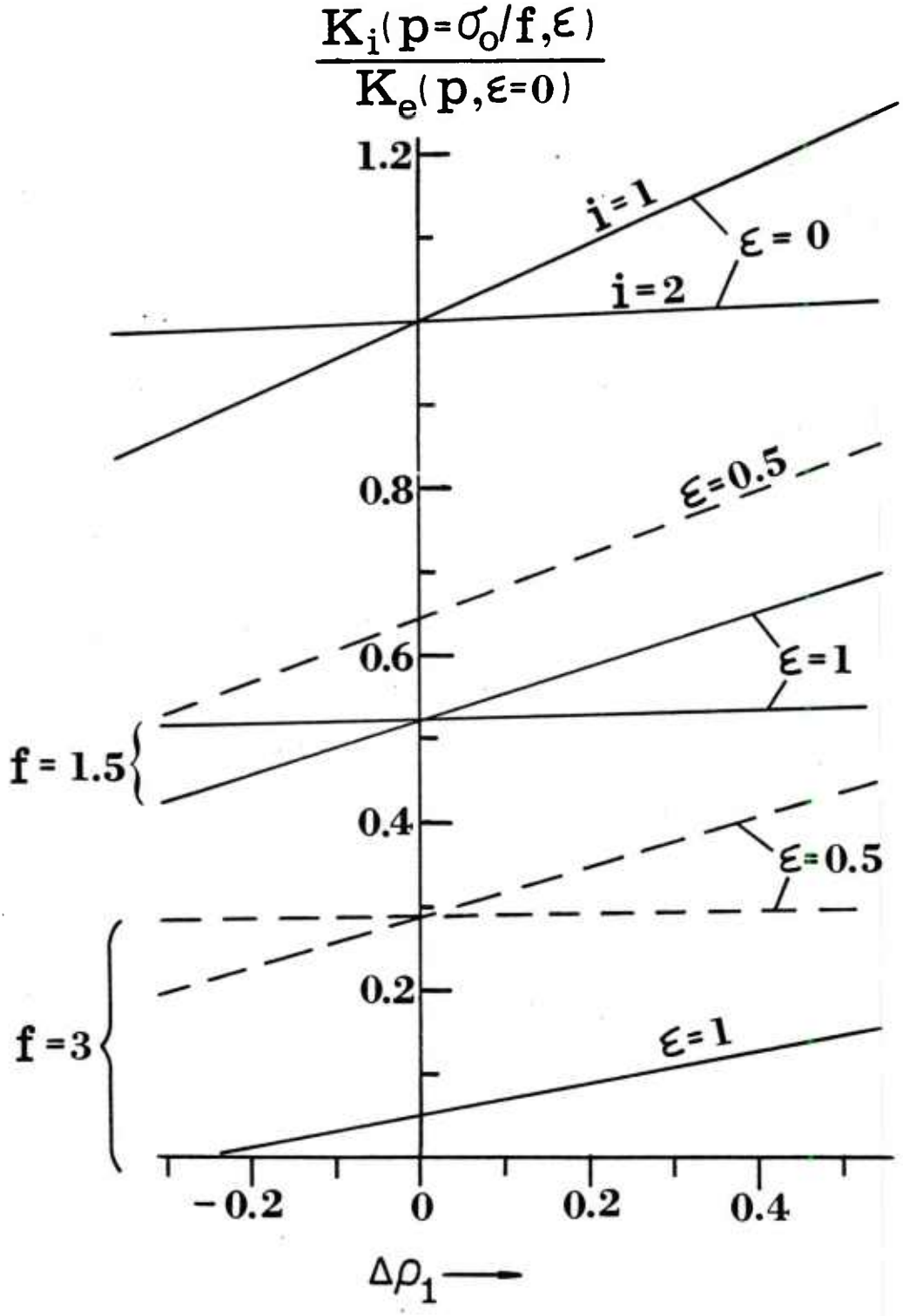

Figure 7. Normalized stress intensity factors as a function of relative change in one of the crack depths, with the other crack fixed at a depth c = 0.1, in a diametrically opposite cracked cylinder which is autofrettaged to a degree of ε and is subjected to an internal pressure $p = \sigma_o/f$.

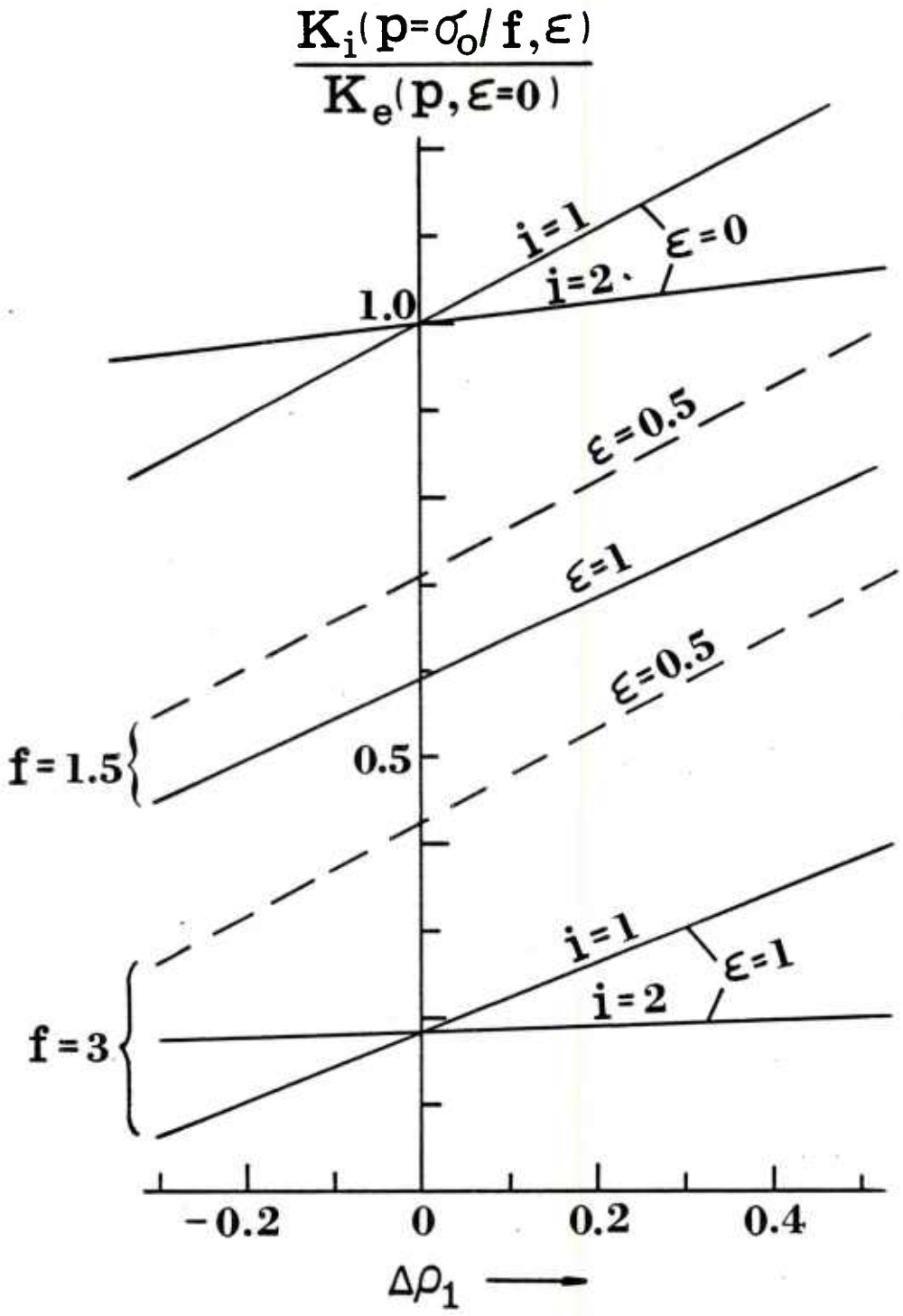

Figure 8. Normalized stress intensity factors as a function of relative change in one of the crack depths, with the other crack fixed at a depth c = 0.2, in a diametrically opposite cracked cylinder which is autofrettaged to a degree of ε and is subjected to an internal pressure $p = \sigma_o/f$.

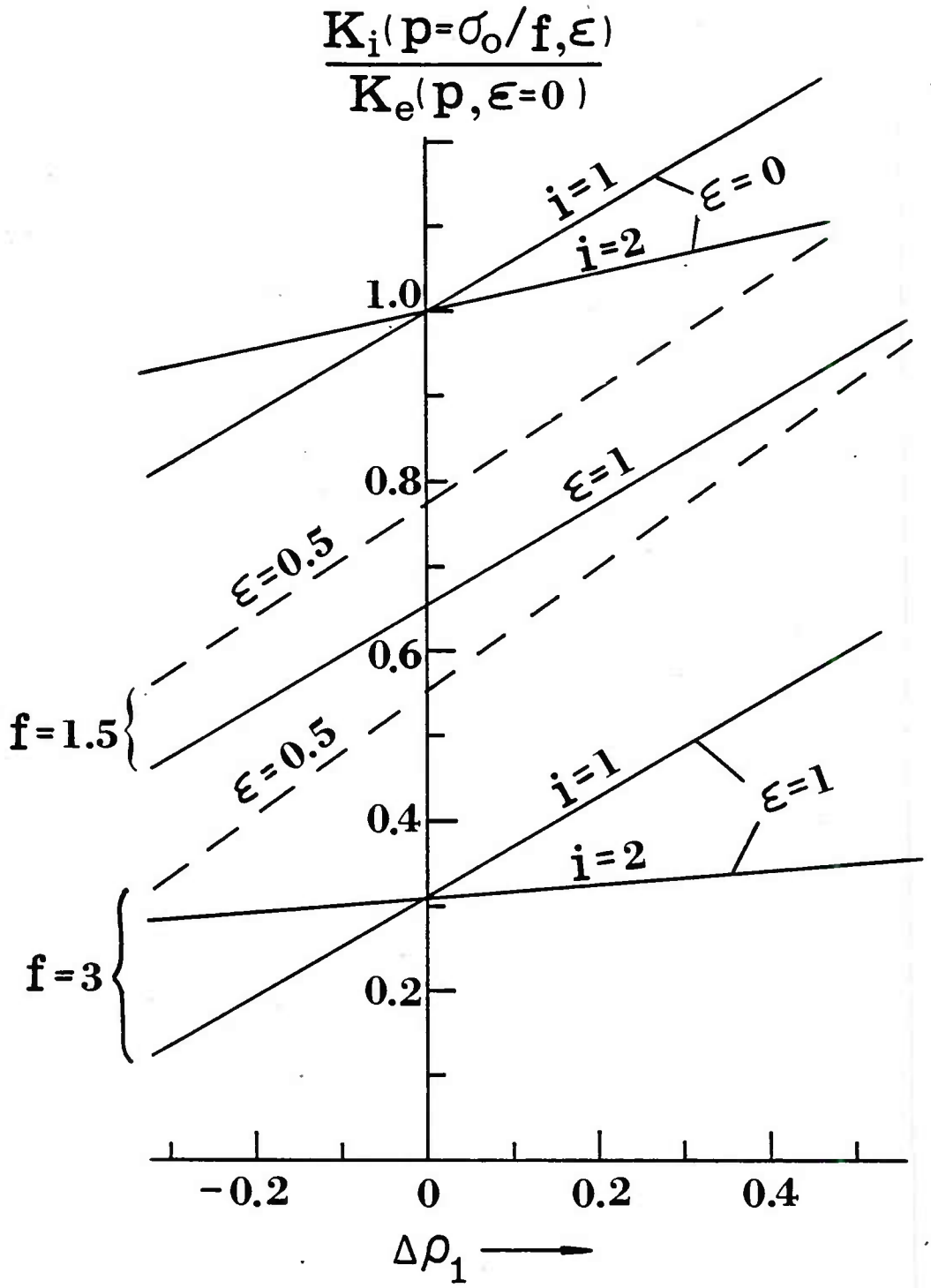

Figure 9. Normalized stress intensity factors as a function of relative change in one of the crack depths, with the other crack fixed at a depth c = 0.3, in a diametrically opposite cracked cylinder which is autofrettaged to a degree of ε and is subjected to an internal pressure $p = \sigma_o/f$.

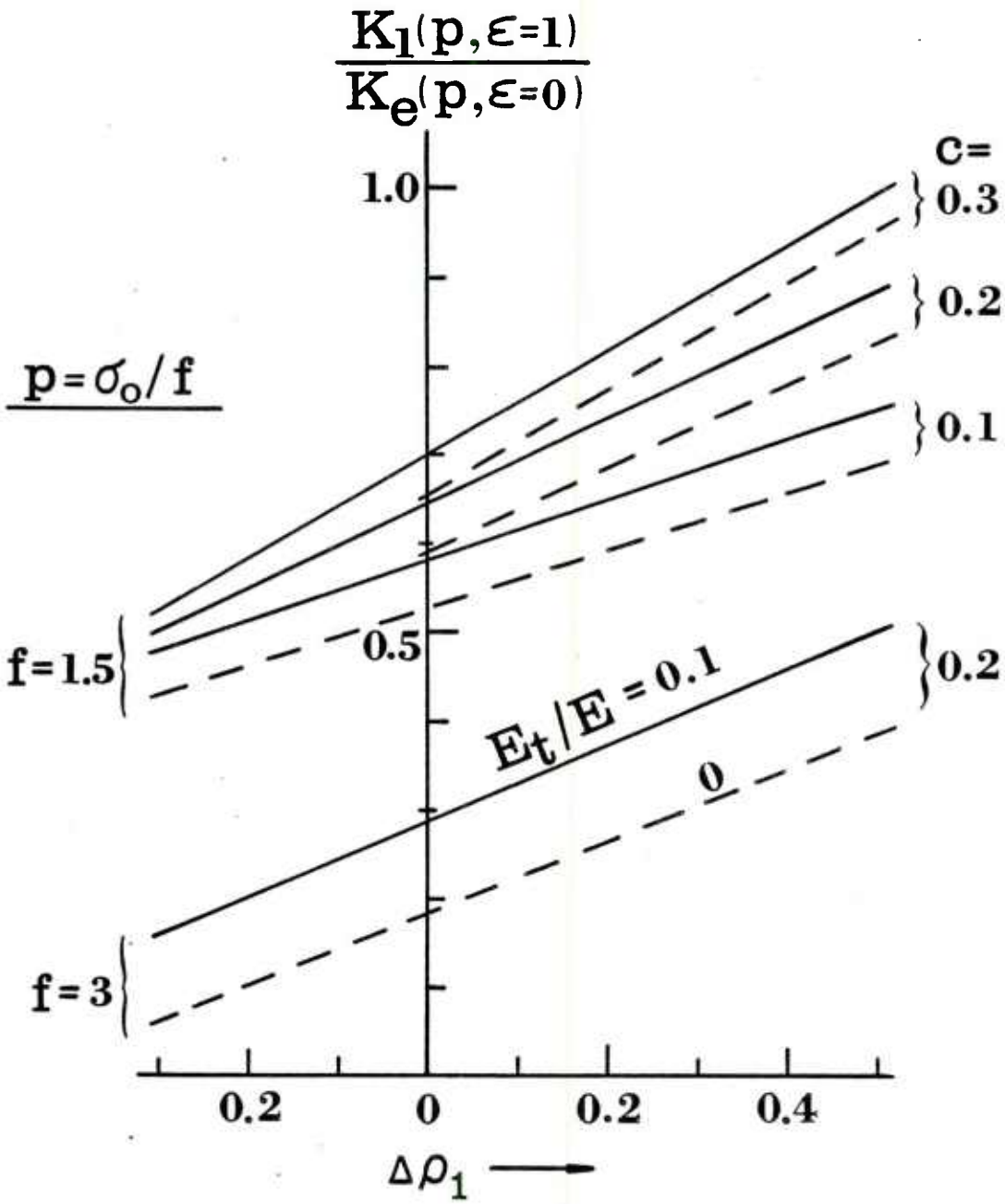

Figure 10. Comparison of normalized stress intensity factors for strain-hardening materials having $E_t = 0.1E$ with corresponding values for elastic-perfectly plastic materials.

TECHNICAL REPORT INTERNAL DISTRIBUTION LIST

	NO. OF COPIES
CHIEF, DEVELOPMENT ENGINEERING BRANCH	
ATTN: SMCAR-LCB-D	1
-DA	1
-DP	1
-DR	1
-DS (SYSTEMS)	1
-DS (ICAS GROUP)	1
-DC	1
CHIEF, ENGINEERING SUPPORT BRANCH	
ATTN: SMCAR-LCB-S	1
-SE	1
CHIEF, RESEARCH BRANCH	
ATTN: SMCAR-LCB-R	2
-R (ELLEN FOGARTY)	1
-RA	1
-RM	2
-RP	1
-RT	1
TECHNICAL LIBRARY	5
ATTN: SMCAR-LCB-TL	
TECHNICAL PUBLICATIONS & EDITING UNIT	2
ATTN: SMCAR-LCB-TL	
DIRECTOR, OPERATIONS DIRECTORATE	1
DIRECTOR, PROCUREMENT DIRECTORATE	1
DIRECTOR, PRODUCT ASSURANCE DIRECTORATE	1

NOTE: PLEASE NOTIFY DIRECTOR, BENET WEAPONS LABORATORY, ATTN: SMCAR-LCB-TL, OF ANY ADDRESS CHANGES.

TECHNICAL REPORT EXTERNAL DISTRIBUTION LIST

	NO. OF COPIES
ASST SEC OF THE ARMY RESEARCH & DEVELOPMENT ATTN: DEP FOR SCI & TECH THE PENTAGON WASHINGTON, D.C. 20315	1
COMMANDER DEFENSE TECHNICAL INFO CENTER ATTN: DTIC-DDA CAMERON STATION ALEXANDRIA, VA 22314	12
COMMANDER US ARMY MAT DEV & READ COMD ATTN: DRCDE-SG 5001 EISENHOWER AVE ALEXANDRIA, VA 22333	1
COMMANDER ARMAMENT RES & DEV CTR US ARMY AMCCOM ATTN: SMCAR-LC	1
SMCAR-LCE	1
SMCAR-LCM (BLDG 321)	1
SMCAR-LCS	1
SMCAR-LCU	1
SMCAR-LCW	1
SMCAR-SCM-O (PLASTICS TECH EVAL CTR, BLDG. 351N)	1
SMCAR-TSS (STINFO) DOVER, NJ 07801	2
DIRECTOR BALLISTICS RESEARCH LABORATORY ATTN: AMXBR-TSB-S (STINFO) ABERDEEN PROVING GROUND, MD 21005	1
MATERIEL SYSTEMS ANALYSIS ACTV ATTN: DRXSY-MP ABERDEEN PROVING GROUND, MD 21005	1
COMMANDER US ARMY AMCCOM ATTN: SMCAR-ESP-L ROCK ISLAND, IL 61299	1
COMMANDER ROCK ISLAND ARSENAL ATTN: SMCRI-ENM (MAT SCI DIV) ROCK ISLAND, IL 61299	1
DIRECTOR US ARMY INDUSTRIAL BASE ENG ACTV ATTN: DRXIB-M ROCK ISLAND, IL 61299	1
COMMANDER US ARMY TANK-AUTMV R&D COMD ATTN: TECH LIB - DRSTA-TSL WARREN, MI 48090	1
COMMANDER US ARMY TANK-AUTMV COMD ATTN: DRSTA-RC WARREN, MI 48090	1
COMMANDER US MILITARY ACADEMY ATTN: CHMN, MECH ENGR DEPT WEST POINT, NY 10996	1
US ARMY MISSILE COMD REDSTONE SCIENTIFIC INFO CTR ATTN: DOCUMENTS SECT, BLDG. 4484 REDSTONE ARSENAL, AL 35898	2
COMMANDER US ARMY FGN SCIENCE & TECH CTR ATTN: DRXST-SD 220 7TH STREET, N.E. CHARLOTTESVILLE, VA 22901	1

NOTE: PLEASE NOTIFY COMMANDER, ARMAMENT RESEARCH AND DEVELOPMENT CENTER, US ARMY AMCCOM, ATTN: BENET WEAPONS LABORATORY, SMCAR-LCB-TL, WATERVLIET, NY 12189, OF ANY ADDRESS CHANGES.

TECHNICAL REPORT EXTERNAL DISTRIBUTION LIST (CONT'D)

	NO. OF COPIES
COMMANDER US ARMY MATERIALS & MECHANICS RESEARCH CENTER ATTN: TECH LIB - DRXMR-PL WATERTOWN, MA 01272	2
COMMANDER US ARMY RESEARCH OFFICE ATTN: CHIEF, IPO P.O. BOX 12211 RESEARCH TRIANGLE PARK, NC 27709	1
COMMANDER US ARMY HARRY DIAMOND LAB ATTN: TECH LIB 2800 POWDER MILL ROAD ADELPHIA, MD 20783	1
COMMANDER NAVAL SURFACE WEAPONS CTR ATTN: TECHNICAL LIBRARY CODE X212 DAHLGREN, VA 22448	1
DIRECTOR US NAVAL RESEARCH LAB ATTN: DIR, MECH DIV	1
CODE 26-27, (DOC LIB) WASHINGTON, D.C. 20375	1
COMMANDER AIR FORCE ARMAMENT LABORATORY ATTN: AFATL/DLJ	1
AFATL/DLJG EGLIN AFB, FL 32542	1
METALS & CERAMICS INFO CTR BATTELLE COLUMBUS LAB 505 KING AVENUE COLUMBUS, OH 43201	1

NOTE: PLEASE NOTIFY COMMANDER, ARMAMENT RESEARCH AND DEVELOPMENT CENTER, US ARMY AMCCOM, ATTN: BENET WEAPONS LABORATORY, SMCAR-LCB-TL, WATERVLIET, NY 12189, OF ANY ADDRESS CHANGES.